Hindawi Publishing Corporation
Mathematical Problems in Engineering
Volume 2015, Article ID 589184, 10 pages
http://dx.doi.org/10.1155/2015/589184

Research Article

Optimal Controller and Controller Based on Differential Flatness in a Linear Guide System: A Performance Comparison of Indexes

Fabio Abel Gómez Becerra,[1,2] Víctor Hugo Olivares Peregrino,[1] Andrés Blanco Ortega,[1] and Jesús Linares Flores[3]

[1]*Centro Nacional de Investigación y Desarrollo Tecnológico, 62490 Cuernavaca, MOR, Mexico*
[2]*ITS de PV, 48333 Puerto Vallarta, JAL, Mexico*
[3]*Universidad Tecnológica de la Mixteca, 69000 Huajuapam de León, OAX, Mexico*

Correspondence should be addressed to Fabio Abel Gómez Becerra; fabioabelgo@hotmail.com

Received 27 August 2015; Revised 20 November 2015; Accepted 23 November 2015

Academic Editor: Wenguang Yu

The use of linear slide system has been augmented in recent times due to features granted to supplement electromechanical systems; new technologies have allowed the manufacture of these systems with low coefficients of friction and offer a variety of types of sliding. In this paper, we present a comparison between the performance indexes of two techniques of control applying optimal control LQR (Linear Quadratic Regulator) acronym for STIs in English and the technique of differential flatness controller. The use of linear slide bolt of potency takes into account the dynamics of the DC motor; the Euler-Lagrange formalism was used to establish the mathematical model of the slide. Cosimulation via the MATLAB/Simulink-ADAMS virtual prototype package, including realistic measurement disturbances, is used to compare the performance indexes between the LQR controller versus differential flatness controller for the position tracking of linear guide system.

1. Introduction

The linear slides have been used in different electromechanical systems as actuators; these have great advantages, especially those consisting of screws-and-nuts; some advantages are as follows: the effect of gravity at the beginning of the movement introduces no disturbance of change of position by not overcoming the power screw, the degree of accuracy in positioning is very high, it is possible to track both soft paths laws of classic and modern control, and the force developed by using this type of device is very high usually requiring actuators (DC motor) of lower power than those requiring other types of systems. Blanco Ortega et al. [1] proposed a rehabilitation ankle device based on an XY table which uses two linear slidings, one on each axis, through a Generalized Proportional Integral (GPI) controller. Valdivia et al. [2] proposed a rehabilitation ankle TobiBot, which covers only the movements of dorsiflexion/plantarflexion, and a degree of freedom; it is controlled by an outline of PID control, to perform the movements, and uses a linear slide based on a power screw. Blanco Ortega et al. [3, 4] in turn presented a rehabilitation of the design and construction of an ankle rehabilitation based on a parallel robot of 3 degrees of freedom, which provides the movements of dorsiflexion/plantarflexion and inversion/eversion made by the ankle and uses a PID control technique to perform rehabilitation ankle movements by using three linear power sliding screws. Blanco Ortega et al. [3, 4] have presented an ankle rehabilitation machine, using a linear slide to effect movements dorsiflexion/ankle plantarflexion; the control technique using a PID was smooth trajectory tracking.

As can be seen, linear slides have been widely used as actuators in various robotic devices from a simple XY table. Various control techniques have been implemented for

accurate position with smooth tracking paths. The present work proposes control technique for differential flatness, compared with optimal control, showing both its advantages and disadvantages over the other, considering the control technique for differential flatness as an option with highly acceptable results in tracking soft paths, and highlighting also the lack of optimization for optimum control trajectories mechanical tracking systems of this type; the randomness of the matrix appears when weighing matrixes R and Q. Control technique by feedback employed in this work is based on the concept of differential flatness, which come from differential plan systems (Fliess et al. [5]). This was made known fifteen years ago in France by professor Fliess and his collaborators. Differential flatness has had important uses within the areas of robotics, control processes, aerospace systems, optimization systems, trajectory planning in linear and nonlinear aspects, and systems of infinite dimensions described in partially controlled differential equations with border conditions (Fliess et al. [5, 6]; Linares-Flores and Sira-Ramírez [7]; and Sira-Ramírez and Agrawal [8]). Thounthong et al. [9] suggest the use of a differential based on flatness of a fuel cell system and a hybrid supercapacitors source achieving robustness, stability, and efficiency of the controlled system controller. Jörgl and Gattringer [10] proposed the control of a conveyor belt using a control law based on differential flatness reducing the trajectory tracking error compared with traditional drivers, flatness theory has been used in a variety of nonlinear systems in various engineering disciplines, Thounthong and Pierfederici [11], such as the inverted pendulum control and aircraft vertical rise and fall, Fliess et al. [12]. Danzer et al. [13] proposed driver in such a control system of the pressure of a cathode and oxygen excess of a chemical system. Gensior et al. [14] used a control of tracking of a DC voltage boost converter. Song et al. [15] have shown that based on flatness control is robust and provides improved performance monitoring transience compared to a traditional method of linear control (PI). A nonlinear system is flat if there is a set of independent variables (differentially equal in number to the number of entries) so that all the state variables x and input variables u can be expressed in terms of those output by Syed et al. [16], Rabbani et al. [17], and Agrawal et al. [18].

In order to make a comparison between the performance index of different controllers, this paper also presents an optimal control law applied to the same linear slide (Figure 1); optimal control theory focuses on the design of controllers to perform their objective and concurrently satisfy physical constraints to optimize predetermined performance criteria (Hassani and Lee [19]). With the new trend of seeking a high-performance, sustainable manufacturing, pollution awareness and finding ways for greater energy efficiency, greater emphasis on the optimal design of control systems is made. The optimality design criteria may include minimum fuel, low energy, minimum time (Lewis [20]). Because of this the focus in recent years has been directed to the use of various techniques of optimal control; Yu and Hwang [21] have presented an LQR (Linear Quadratic Regulator) approach for determining a control law PID optimal in order to control the speed of a DC motor; this contribution proposes a systematic approach to design a speed control of a DC motor based on an identification model and LQR design with a nonlinear increase with feedforward compensator. Ruderman et al. [22] propose a methodical approach LQR state feedback control of a DC motor. Likewise LQR optimal control has been used in conjunction with other control techniques such as that of Prasad et al. [23] who proposed a control system high nonlinearity such as the inverted pendulum. It is presented with a linearized dynamics using a PID controller LQR bringing out results in a robust control scheme for optimal system control.

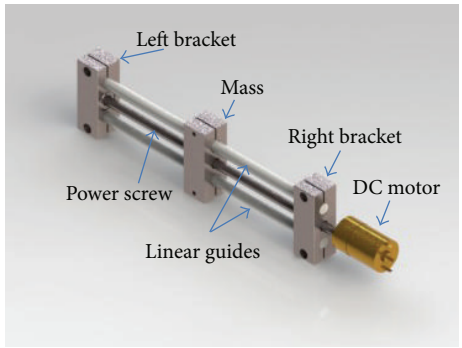

Figure 1: Linear slide system.

The contributions of this paper are as follows: (1) the design of an LQR position tracking controller; (2) the design of a differential flatness position tracking controller; these tracking controllers are compared on the performance index of position tracking error. Thus, we conclude that the two controllers have a high capacity for the position tracking of the linear guide system. This paper is organized as follows. Section 2 presents the mathematical model of linear slide system. In this section, we obtained the mathematical model via Euler-Lagrange formalism and incorporate the dynamic of DC motor to model. The position control based on linear quadratic regulator is presented in Section 3. In Section 4, we present the design of tracking controller based on differential flatness. In Section 5, the simulations results are obtained through the MATLAB/Simulink-ADAMS virtual prototype package, and we compare the performance indexes of the position tracking error of both controllers. In Section 6, the results are shown in the experiment using a physical slider and data acquisition card, using the LabView software with a graphical interface. Finally, in Section 7, we give the conclusions of all of the work.

2. Mathematical Model of Linear Slide

The linear slide control in this work is formed with a motor coupled CD to a power screw through a gearbox speed, screw, and rotating, linearly moving mass m, as shown in Figures 1 and 2.

Motor mathematical model of linear guide system was obtained by applying the Euler-Lagrange formalism. It considers the dynamics of the DC motor. The generalized coordinates are q and θ.

Consider Figure 2 and the notation shown in Notation.

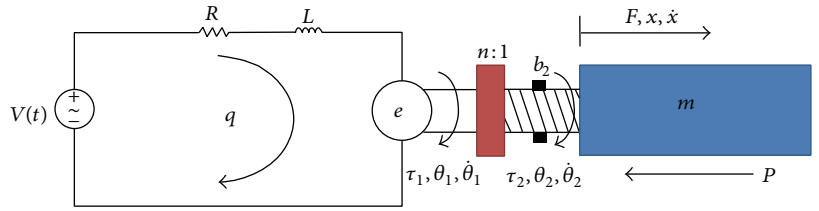

Figure 2: Schematic diagram of a linear slide system-DC motor.

2.1. Electric Motor. Considering Figure 2, the coenergy by storage of effort is given by (1), the coenergy storage of effort by (2), and the energy dissipation by (3).

Coenergy by Storage of Effort. Consider

$$T^* = \frac{1}{2}L\dot{q}^2. \tag{1}$$

The Storage of Energy Flow. Consider

$$U = 0. \tag{2}$$

Energy Dissipation. Consider

$$G = \frac{1}{2}R\dot{q}^2. \tag{3}$$

2.2. Linear Slide. The kinetic energy of the system of linear slide is given by (4) and the dissipated energy is represented by (7).

Kinetic Energy. Consider

$$K = \frac{1}{2}I\dot{\theta}_2^2 + \frac{1}{2}m\dot{x}^2. \tag{4}$$

Knowing that $x = p\theta_2$, $\dot{x} = p\dot{\theta}_2$, and $\ddot{x} = p\ddot{\theta}_2$ and substituting in (4), the following equation is obtained, with kinetic energy remaining in function of the angular velocity of the power screw (see Figure 2):

$$K = \frac{1}{2}I\dot{\theta}_2^2 + \frac{1}{2}m\left(p\dot{\theta}_2\right)^2. \tag{5}$$

Dissipated Energy. Consider

$$D = \frac{1}{2}b_2\dot{\theta}_2^2. \tag{6}$$

From (1) until (5) is represented total system in the kinetic energy and the following equation is obtained:

$$K_T = \frac{1}{2}L\dot{q}^2 + \frac{1}{2}I\dot{\theta}_2^2 + \frac{1}{2}m\left(p\dot{\theta}_2\right)^2, \tag{7}$$

where L is the Lagrangian and is given by

$$L = \frac{1}{2}L\dot{q}^2 + \frac{1}{2}I\dot{\theta}_2^2 + \frac{1}{2}m\left(p\dot{\theta}_2\right)^2. \tag{8}$$

For the generalized coordinate q,

$$\begin{aligned} \frac{\partial L}{\partial \dot{q}} &= L\dot{q}, \\ \frac{d}{dt}\frac{\partial L}{\partial \dot{q}} &= L\ddot{q}, \\ \frac{\partial L}{\partial q} &= 0, \\ \frac{\partial D}{\partial \dot{q}} &= R\dot{q}, \end{aligned} \tag{9}$$

where

$$L\ddot{q} + R\dot{q} = V(t) - e. \tag{10}$$

Considering that $e = k_b\dot{\theta}_1$ and $\dot{\theta}_1 = n\dot{\theta}_2$ as well as $\dot{\theta}_2 = \dot{x}/p$ and replacing them in (10), the following equation is obtained:

$$L\ddot{q} + R\dot{q} = V(t) - k_b\left(\frac{n}{p}\right)\dot{x}. \tag{11}$$

Knowing that

$$q = \int_0^t i\,dt, \tag{12}$$

the following equation is obtained:

$$L\frac{di}{dt} + Ri = V(t) - k_b\left(\frac{n}{p}\right)\dot{x}. \tag{13}$$

For the generalized coordinate θ_2,

$$\begin{aligned} \frac{\partial L}{\partial \dot{\theta}_2} &= I\dot{\theta}_2 + mp\dot{\theta}_2, \\ \frac{d}{dt}\frac{\partial L}{\partial \dot{\theta}_2} &= I\ddot{\theta}_2 + mp\ddot{\theta}_2, \\ \frac{\partial L}{\partial \theta_2} &= 0, \\ \frac{\partial D}{\partial \dot{\theta}_2} &= b_2\dot{\theta}_2. \end{aligned} \tag{14}$$

Equation of Euler-Lagrange formalism is

$$\frac{d}{dt}\frac{\partial L}{\partial \dot{q}_i} - \frac{\partial L}{\partial q_i} + \frac{\partial D}{\partial \dot{q}_i} = \tau, \quad \text{to } i = 1, 2, \ldots, n. \tag{15}$$

The mathematical model of the linear slide taking into account the dynamics of the DC motor is defined by

$$L\frac{di}{dt} + Ri = V(t) - k_b\left(\frac{n}{p}\right)\dot{x}, \tag{16}$$

$$\left(\frac{I}{p} + mp\right)\ddot{x} + \frac{b_2}{p}\dot{x} = nk_f i - P. \tag{17}$$

3. Optimal Control

3.1. Considering Acceleration State Variable. Based on the mathematical model (16) and (17), i is derived and from (17) it is clear that

$$\begin{aligned} i &= \left(\frac{\alpha}{nk_f}\right)\ddot{x} + \left(\frac{b_2}{pnk_f}\right)\dot{x}, \\ \frac{di}{dt} &= \left(\frac{\alpha}{nk_f}\right)\dddot{x} + \left(\frac{b_2}{pnk_f}\right)\ddot{x}. \end{aligned} \tag{18}$$

Substituting in (16), one has

$$\begin{aligned} L\left(\frac{\alpha}{nk_f}\right)\dddot{x} + \left(\frac{b_2}{pnk_f}\right)\ddot{x} + R\left(\frac{\alpha}{nk_f}\right)\ddot{x} + \left(\frac{b_2}{pnk_f}\right)\dot{x} \\ = V(t) - K_b\left(\frac{n}{p}\right)\dot{x}. \end{aligned} \tag{19}$$

Fixing the equation, one gets

$$\begin{aligned} L\left(\frac{\alpha}{nk_f}\right)\dddot{x} + \left(\frac{b_2}{pnk_f} + \frac{R\alpha}{nk_f}\right)\ddot{x} + \left(\frac{b_2}{pnk_f} + \frac{k_b n}{p}\right)\dot{x} \\ = u. \end{aligned} \tag{20}$$

The state variables are

$$\begin{aligned} \dot{x}_1 &= x_2, \\ \dot{x}_2 &= x_3, \\ \dot{x}_3 &= -\left(\frac{nk_f}{L\alpha}\right)\left(\frac{b_2}{pnk_f} + \frac{k_b n}{p}\right)\dot{x} \\ &\quad -\left(\frac{nk_f}{L\alpha}\right)\left(\frac{b_2}{pnk_f} + \frac{R\alpha}{nk_f}\right)\ddot{x} + \frac{nk_f}{L\alpha}u. \end{aligned} \tag{21}$$

Placing the state variables in the matrix form, one gets

$$\begin{aligned} \dot{x} &= Ax + Bu, \\ y &= Cx, \\ \begin{vmatrix} \dot{x}_1 \\ \dot{x}_2 \\ \dot{x}_3 \end{vmatrix} &= \begin{vmatrix} 0 & 1 & 0 \\ 0 & 0 & 1 \\ 0 & -\left(\frac{nk_f}{L\alpha}\right)\left(\frac{b_2}{pnk_f} + \frac{k_b n}{p}\right) & -\left(\frac{nk_f}{L\alpha}\right)\left(\frac{b_2}{pnk_f} + \frac{R\alpha}{nk_f}\right) \end{vmatrix} \begin{vmatrix} x_1 \\ x_2 \\ x_3 \end{vmatrix} + \begin{vmatrix} 0 \\ 0 \\ \frac{nk_f}{L\alpha} \end{vmatrix} u, \\ y &= \begin{pmatrix} 1 & 0 & 0 \end{pmatrix}\begin{pmatrix} x_1 \\ x_2 \\ x_3 \end{pmatrix}. \end{aligned} \tag{22}$$

In control systems, often we want to select the control vector $u(t)$ such that a given performance index is minimized. A quadratic performance index, where the integration limits are 0 to ∞, so that

$$J = \int_0^\infty L(x, u)\, dt, \tag{23}$$

where $L(x, u)$ is a quadratic function or a Hermitian function of x and u, produces linear control laws; that is to say,

$$u = -Kx(t). \tag{24}$$

For weight matrixes for semipositive definite Q and R, the optimal control system is based on minimizing the performance index. This requires numerically solving the Riccati algebraic equation:

$$A^T P + PA - PBR^{-1}B^T P + Q = 0 \tag{25}$$

for a symmetric positive definite matrix P.

Finally, gains are calculated as

$$K = R^{-1}B^T P. \tag{26}$$

In the present case, u is given by

$$u = -k_1 x_1 - k_2 x_2 - k_3 x_3. \tag{27}$$

The state weighting matrix is proposed as

$$Q = C^T C,$$

$$Q = \begin{pmatrix} 1 \\ 0 \\ 0 \end{pmatrix} \begin{pmatrix} 1 & 0 & 0 \end{pmatrix} = \begin{pmatrix} 1 & 0 & 0 \\ 0 & 0 & 0 \\ 0 & 0 & 0 \end{pmatrix} \tag{28}$$

which meets nonnegative definite. As for the scalar weighting for the control input, it is chosen as

$$R = 0.01, \quad R = 1e - 10. \tag{29}$$

3.2. Considering State Variable Motor Current CD. By representing mathematical model equations (16) and (17) in state space, one gets

$$\dot{x}_1 = x_2,$$

$$\alpha \dot{x}_2 = -\frac{b_2}{p} x_2 + n k_f x_3,$$

$$L \dot{x}_3 = -R x_3 - \left(\frac{n k_b}{p} \right) x_2 + u(t),$$

$$\begin{vmatrix} \dot{x}_1 \\ \dot{x}_2 \\ \dot{x}_3 \end{vmatrix} = \begin{vmatrix} 0 & 1 & 0 \\ 0 & -\dfrac{b_2}{\alpha p} & \dfrac{n k_f}{\alpha} \\ 0 & -\dfrac{n k_b}{L p} & -\dfrac{R}{L} \end{vmatrix} \begin{vmatrix} x_1 \\ x_2 \\ x_3 \end{vmatrix} + \begin{vmatrix} 0 \\ 0 \\ \dfrac{1}{L} \end{vmatrix} u, \tag{30}$$

$$C = \begin{vmatrix} 1 & 0 & 0 \end{vmatrix},$$

$$D = |0|,$$

$$Q = \begin{pmatrix} 1 \\ 0 \\ 0 \end{pmatrix} \begin{pmatrix} 1 & 0 & 0 \end{pmatrix} = \begin{pmatrix} 1 & 0 & 0 \\ 0 & 0 & 0 \\ 0 & 0 & 0 \end{pmatrix}$$

with

$$R = 0.01 \tag{31}$$

for the first case and

$$R = 1e - 10 \tag{32}$$

for the second case.

3.3. LQR Optimal Control in Virtual Prototype. A test was performed using a virtual prototype of the linear slide, Figure 3, in room ADAMS MSC together with Matlab-Simulink in order to test the effectiveness of optimal control LQR; the results of this experiment can be seen in Section 5.

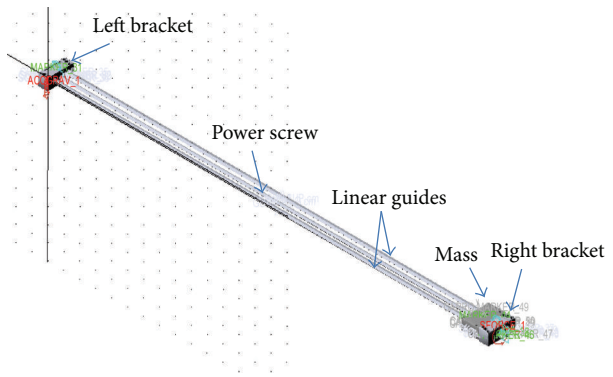

Figure 3: Virtual prototype of the linear slide.

4. Control Based on Differential Flatness

This third-order linear system (30), where its Kalman controllability matrix is calculated by the following expression: $C = [B, AB, A^2B]$, is given as

$$C = \begin{vmatrix} 0 & 0 & \dfrac{n k_f}{\alpha} \\ 0 & \dfrac{n k_f}{\alpha} & -\dfrac{R n k_f}{L\alpha} - \dfrac{n b_2 k_f}{p\alpha^2} \\ 1 & -\dfrac{R}{L} & \dfrac{R^2}{L^2} - \dfrac{n^2 k_b k_f}{Lp\alpha} \end{vmatrix} \quad \det C = -\frac{n^2 k_f^2}{\alpha^2} \neq 0. \tag{33}$$

Since the determinant is nonzero, then the system is controllable and, therefore, is differentially flat (Sira-Ramírez and Agrawal [8]). The flat output of a linear system input output (I/O) is obtained by multiplying the inverse matrix of controllability by the state vector x, associated with the system. Column vector obtained by multiplying the last line is chosen to obtain the flat output (Linares-Flores and Sira-Ramírez [7]). In particular for reducing motor-drive CD, flat output system F is calculated as

$$F = \begin{vmatrix} 0 & 0 & 1 \end{vmatrix} C^{-1} \begin{vmatrix} x_1 \\ x_2 \\ x_3 \end{vmatrix},$$

$$F = \begin{vmatrix} 0 & 0 & 1 \end{vmatrix} \begin{vmatrix} \dfrac{\left(k_b k_f n^2 + R b_2\right)}{L n p k_f} & \dfrac{R\alpha}{L n k_f} & 1 \\ \dfrac{\left(L b_2 + R p \alpha\right)}{L n p k_f} & \dfrac{\alpha}{n k_f} & 0 \\ \dfrac{\alpha}{n k_f} & 0 & 0 \end{vmatrix} \begin{vmatrix} x_1 \\ x_2 \\ x_3 \end{vmatrix} \tag{34}$$

$$= \frac{\alpha}{n k_f} x_1.$$

Table 1: Parameter values for simulation.

Parameter	Value
n = speed ratio	0.19
P = force opposite to the movement of m	0.01 N
b_2 = coefficient of viscous friction	2
p = pitch of the screw thread power	0.00196 m
m = mass to be displaced	10 kg
J = moment of inertia	0.0000014 kg m^2
V = voltage	12 volts
k_b = constant emf	0.022 (Vs)/rad
R = resistance of DC motor	5.3 ohm
L = motor inductance	0.00058 henries
K_f = constant torque	90 (N-m)/A

Hence, we have chosen x_1 as the flat output. This flat output provides the following differential parametrization of the system variables:

$$\begin{aligned} x_1 &= F, \\ x_2 &= \dot{F}, \\ x_3 &= \left(\frac{\alpha}{nk_f}\right)\ddot{F} + \left(\frac{b_2}{nk_f p}\right)\dot{F} + \frac{P}{nk_f p}, \end{aligned} \tag{35}$$

and the control input:

$$\begin{aligned} u = {} & \left[\frac{L\alpha}{nk_f}\right]\dddot{F} + \left[\frac{Lb_2}{nk_f p} + \frac{R\alpha}{nk_f}\right]\ddot{F} \\ & + \left[\frac{Rb_2}{nk_f p} + \frac{nk_b}{p}\right]\dot{F} + \frac{RP}{nk_f p}. \end{aligned} \tag{36}$$

Considering (36) and in order to verify the stability of the system, applying the Laplace transform, the following holds:

$$\begin{aligned} u = {} & \left[\frac{L\alpha}{nk_f}\right]s^3 + \left[\frac{Lb_2}{nk_f p} + \frac{R\alpha}{nk_f}\right]s^2 \\ & + \left[\frac{Rb_2}{nk_f p} + \frac{nk_b}{p}\right]s + \frac{RP}{nk_f p}. \end{aligned} \tag{37}$$

Taking into account the values of Table 1, the system transfer function is

$$\begin{aligned} & \frac{F(s)}{u(s)} \\ & \quad = \frac{1}{6.8854 * 10^{-7}s^3 + 4.0902 * 10^{-2}s^2 + 318.40s}. \end{aligned} \tag{38}$$

Plotting the locus of roots verifies that the system is stable when these are in the left half of the complex plane (Figure 4).

Hence, we have the fact that all state variables and the control input are in terms of F and its successive derivatives, where it denotes the position of the mass as x. The differential parametrization above allows obtaining the equilibrium for

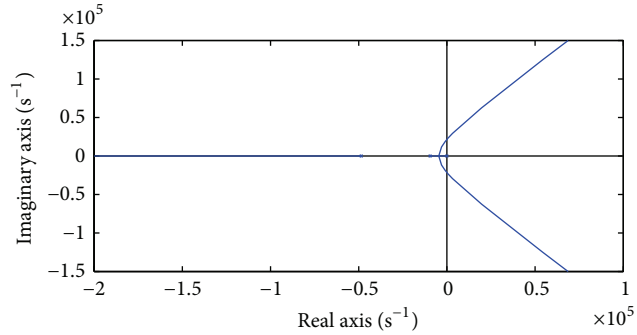

Figure 4: Roots locus.

the system in terms of the equilibrium values of the flat output and the disturbance inputs. Thus,

$$\begin{aligned} \overline{x}_1 &= \overline{F}_d, \\ \overline{x}_2 &= 0, \\ \overline{x}_3 &= \frac{\overline{P}}{nk_f p}, \\ \overline{u} &= \frac{R\overline{P}}{nk_f p}. \end{aligned} \tag{39}$$

From (36), we design the average controller based on differential flatness property. Thus, we replace the higher-order derivative of the flat output by a virtual controller (see Slotine and Li [24]) resulting in the following:

$$\dddot{\overline{F}} = v_{\text{aux}} = -k_2\ddot{F} - k_1\dot{F} - k_0\left(F - \overline{F}_d\right). \tag{40}$$

For the tracking controller design, we use a nominal desired linear displacement profile F_d that exhibits a rather smooth start for the motor linear slide system. This is specified using an interpolating Bézier polynomial of 10th order where the initial linear displacement is set to be $F_{\text{ini}} = 0$ m valid until $t_{\text{ini}} = 15$ sec and the final desired value of the angular velocity is specified as $F_{\text{fin}} = 0.5$ m to be reached at $t_{\text{fin}} = 45$ sec; that is, we used

$$F_d = \begin{cases} F_{\text{ini}}, & t < t_{\text{ini}}, \\ F_{\text{ini}} + \left(F_{\text{fin}} - F_{\text{ini}}\right)b_x, & t_{\text{ini}} \le t \le t_{\text{fin}}, \\ F_{\text{fin}}, & t > t_{\text{fin}}, \end{cases} \tag{41}$$

where $b_x(t, t_{\text{ini}}, t_{\text{fin}})$ is a polynomial function of time, exhibiting a sufficient number of zero derivatives at times t_{ini} and t_{fin}, while also satisfying $b_x(t_{\text{ini}}, t_{\text{ini}}, t_{\text{fin}}) = 0$ and $b_x(t_{\text{fin}}, t_{\text{ini}}, t_{\text{fin}}) = 1$. For instance, one such polynomial may be given by

$$\begin{aligned} & b_x(t, t_{\text{ini}}, t_{\text{fin}}) \\ & \quad = \beta^5\left[r_1 - r_2\beta + r_3\beta^2 - r_4\beta^3 + r_5\beta^4 - r_6\beta^5\right], \\ & \beta = \left(\frac{t - t_{\text{ini}}}{t_{\text{fin}} - t_{\text{ini}}}\right). \end{aligned} \tag{42}$$

The differential parametrization of the control input, u, in terms of F_d shows that the proposed flat output trajectory tracking task is that of controlling the third derivative of F_d by means of v_{aux}:

$$v_{\text{aux}} = \dddot{F}_d - k_2\left(\ddot{F} - \ddot{F}_d\right) - k_1\left(\dot{F} - \dot{F}_d\right) - k_0\left(F - F_d\right). \quad (43)$$

Therefore, the linear displacement-tracking controller is

$$u = \left[\frac{L\alpha}{nk_f}\right] v_{\text{aux}} + \left[\frac{Lb_2}{nk_f p} + \frac{R\alpha}{nk_f}\right] \ddot{F}_d + \left[\frac{Rb_2}{nk_f p} + \frac{nk_b}{p}\right] \dot{F}_d + \frac{RP}{nk_f p}. \quad (44)$$

Under these circumstances, the closed loop system tracking error, $e = F - F_d$, satisfies the linear differential equation

$$e^{(3)} + k_2\ddot{e} + k_1\dot{e} + k_0 e = 0. \quad (45)$$

The appropriate choice of the constant coefficients $\{k_2, k_1, k_0\}$, as coefficients of the third-order Hurwitz polynomial, guarantees the asymptotic exponential stability to zero of the tracking error, e. One such choice, yielding a characteristic polynomial of the form $(s + \gamma)(s^2 + 2\xi\omega_n s + \omega_n^2)$ with $\gamma > 0$, $0 < \xi < 1$, and $\omega_n > 0$, is given by

$$\begin{aligned} k_0 &= \omega_n^2\gamma, \\ k_1 &= 2\xi\omega_n\gamma + \omega_n^2, \\ k_2 &= 2\xi\omega_n + \gamma. \end{aligned} \quad (46)$$

The virtual controller, v_{aux}, achieves a smooth start for the linear displacement of the system. If we apply an unknown constant load torque on the system, we have to include a term of integral action into the virtual control (43). Thus, we minimize the tracking error near to zero.

5. Simulation Results

These results were obtained using the parameter values of Table 1.

In Figure 5, one can see the movement of the mass 0.5 meters in 60 seconds following a path originated by a tenth-order Bézier polynomial; the tracking error can be seen as zero in the whole path; in this case, the acceleration is taken as a state variable.

Figure 6 shows the graphs of results taking into account the current as state variable; considering the matrix $R = 0.01$ and considering the matrix $R = 1e - 10$, Figure 7, in both cases the tracking error can be seen as zero in the whole path.

Figure 8 shows the results of simulation based on differential flatness controller observed; it also shows that it is capable of moving the mass to a position 0.5 meters along a desired path of a Bézier polynomial of tenth order.

The results of the performance index are as follows: the two controllers are shown in Figures 9, 10, and 11; the indexes of performance of the optimal controller for two values of the matrix R are shown.

Figure 12 shows the results using a virtual prototype environment ADAMS MSC and MATLAB-Simulink; we can see that the offset for this test was set at 0.7 meters corresponding to the desired position; a tenth-order Bézier polynomial was used as desired path.

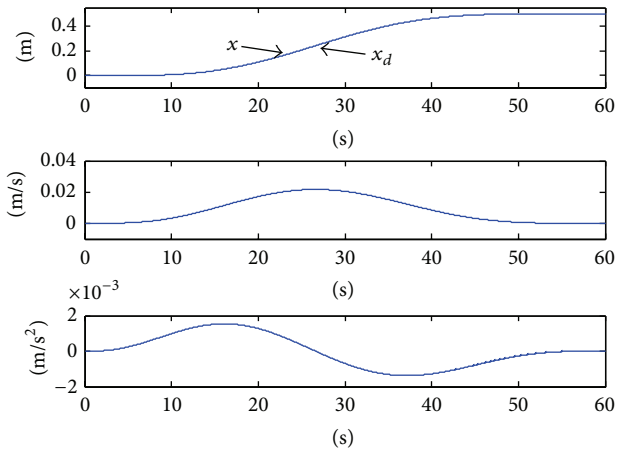

Figure 5: Graphics optimal controller response with $R = 1e - 10$.

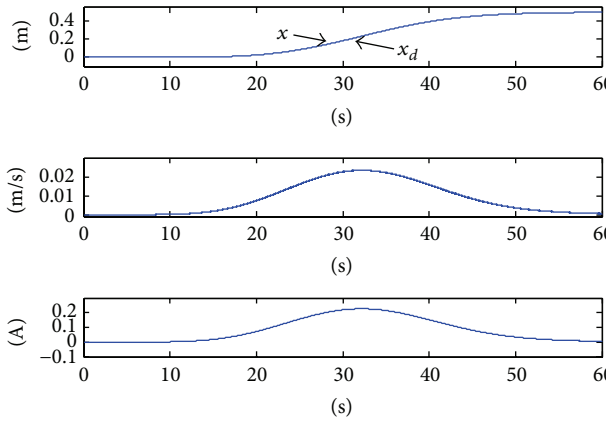

Figure 6: Graphics optimal controller response with $R = 0.01$.

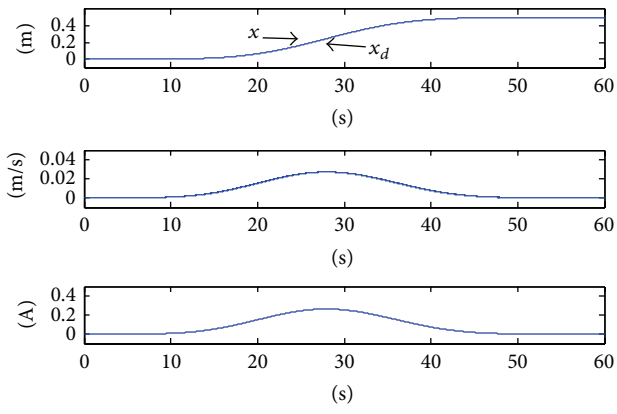

Figure 7: Graphics optimal controller response with $R = 1e - 10$.

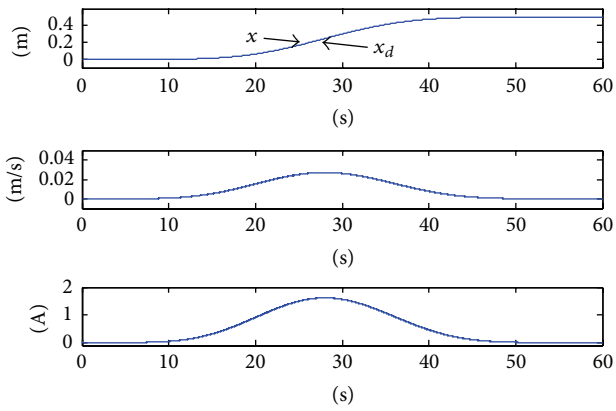

Figure 8: Graphics controller response flatness based on difference.

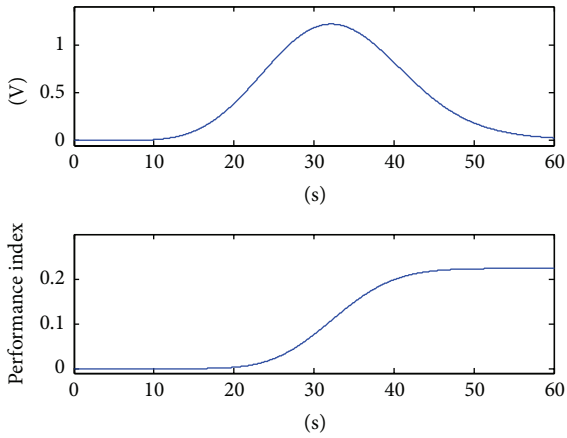

Figure 9: Performance Index LQR optimal controller with $R = 0.01$.

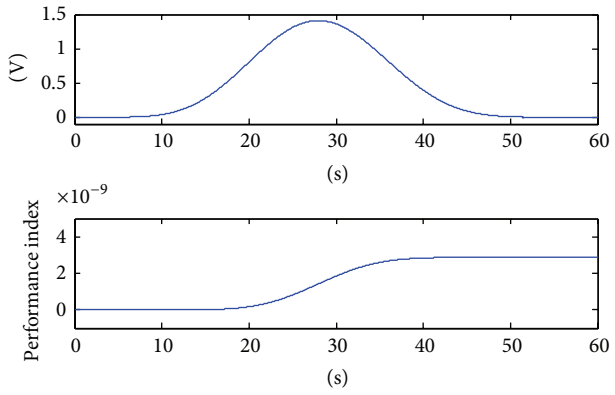

Figure 10: Performance Index LQR optimal controller with $R = 1e-10$.

6. Results with Linear Slide

Experimentation was held using a physical linear slide (Figure 13); the laws of LQR control are implemented based on differential flatness with the same parameter values and gains controllers; the results of the experiment can be seen in Figures 14, 15, and 16, where it can be seen that in all three cases the controller is able to zero the position error; it is clear

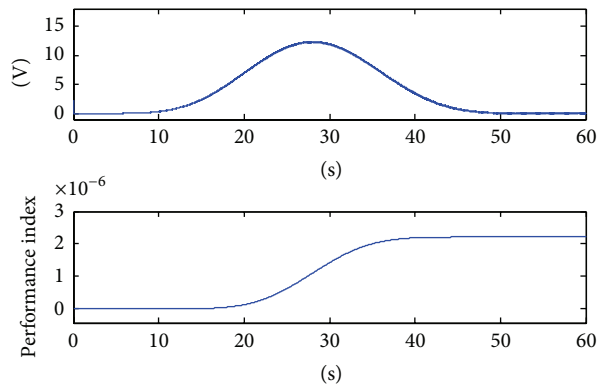

Figure 11: Controller performance index based on differential flatness.

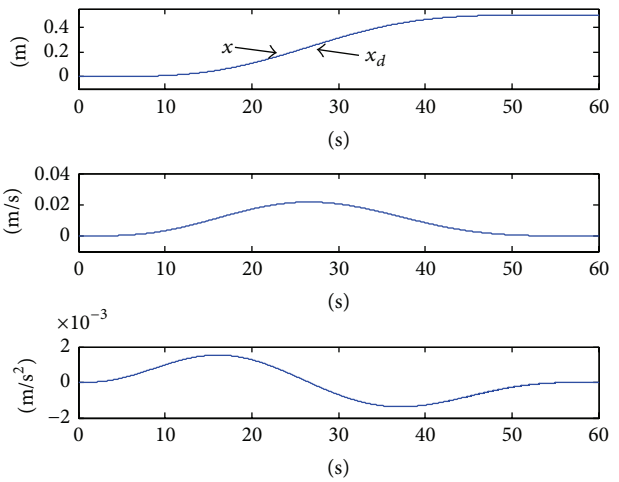

Figure 12: Graphic of LQR optimal controller results in the virtual prototype.

that the experiment was carried out with an acquisition card myRIO data of National Instruments; the measurement units were centimeters so that they should be taken into account in the interpretation of Figures 14, 15, and 16.

It is verified by the results the correct operation for achieving desired trajectories and references.

On the x-axis is the number of samples; to determine the time it must be multiplied by the sampling period, that is, 0.1 s.

7. Conclusions

By applying control techniques and optimal LQR and based on differential flatness it can be seen that the results for the trajectory tracking are highly achievable in both cases, with regard to the performance indices of each controller for the optimal controller; a great disadvantage exists since it is necessary that the values of the weighting matrix R be too low to achieve a speed of response adapted to the needs of the plant to controlling; this means that the gains are higher further input values, such as the voltage that must be adjusted

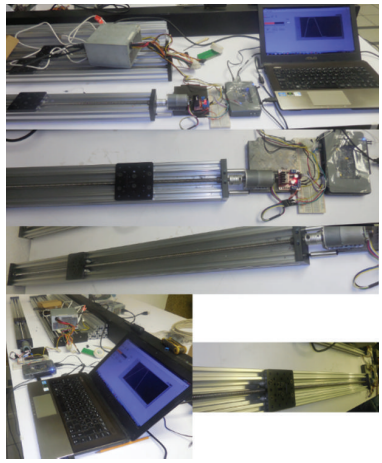

Figure 13: Experiment with physical linear slide.

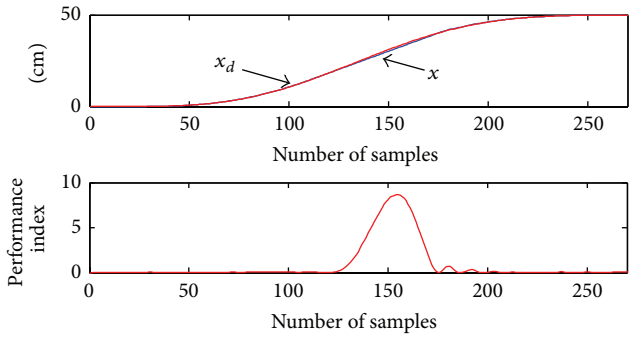

Figure 14: Controller based on differential flatness.

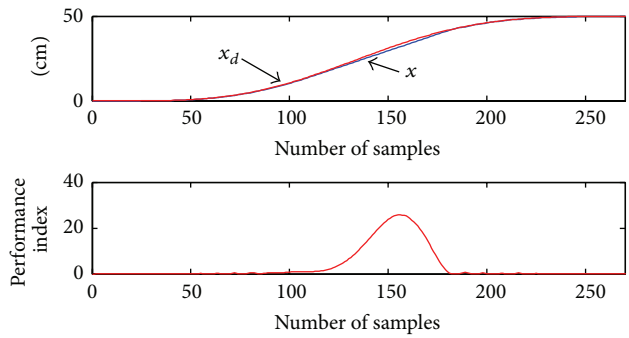

Figure 15: Performance Index LQR optimal controller with $R = 0.01$.

by trial and error of said matrix with the purpose of respecting the voltages of the actuators.

Figures 12 and 13 show that the values of the performance index are minimizing in the measure that the value of the weighting matrix, R, is minor compared to the index controller performance differential flatness, if it is minor, but this is not guaranteed to be optimal because the values of the control force are lower than those required for the good functioning of DC motors.

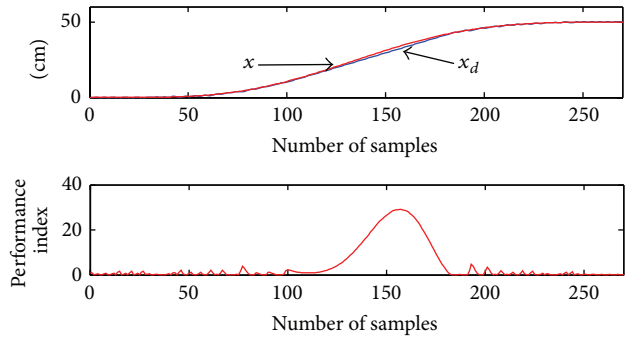

Figure 16: Performance Index LQR optimal controller with $R = 1e-10$.

In conclusion it follows that the use of control laws differential flatness is by far better than the use of laws of optimal control; the concept of optimality, in this particular case, is lost due to the randomness representing search for the value of the R matrix to obtain appropriate response speed without sacrificing system actuators.

Notation

n: Speed ratio
P: Force opposite to the movement of m
b_2: Coefficient of viscous friction
p: Pitch of the screw thread power
m: Mass to be displaced
J: Moment of inertia
V: Voltage
k_b: Constant emf
R: Resistance of DC motor
L: Motor inductance
k_{tao}: Constant torque
θ_1: Angular position of DC motor
$\dot{\theta}_1$: Angular velocity of DC motor
θ_2: Angular position of power screw
$\dot{\theta}_2$: Angular velocity of power screw
τ_1: Torque delivered by the DC motor
τ_2: Torque delivered by the speed reducer
x: Displacement of the mass
$\dot{x}$: Velocity of the mass
F: Force of displacement of the mass.

Conflict of Interests

The authors declare that there is no conflict of interests regarding the publication of this paper.

References

[1] A. Blanco Ortega, F. A. Gómez-Becerra, L. G. Vela Valdés, and R. O. Delgado Arcega, "A generalized proportional integral controller for an ankle rehabilitation machine based on an XY table," in *Proceedings of the IEEE International Conference on Mechatronics, Electronics and Automotive Engineering (ICMEAE '13)*, pp. 152–157, IEEE, Morelos, Mexico, November 2013.

[2] C. H. G. Valdivia, J. L. C. Escobedo, A. B. Ortega, M. A. O. Salazar, and F. A. G. Becerra, "Diseño y control de un sistema interactivo para la rehabilitación de tobillo: TobiBot," *Ingeniería Mecánica. Tecnología y Desarrollo*, vol. 5, no. 1, pp. 255–264, 2014.

[3] A. Blanco Ortega, J. Isidro Godoy, E. Quintero Mármol, and L. G. Vela Valdés, "Robot paralelo para rehabilitación asistida de tobillo," in *X Congreso Internacional sobre Innovación y Desarrollo Tecnológico (CIINDET '13)*, Cuernavaca, Mexico, March 2013.

[4] A. Blanco Ortega, H. R. Azcaray Rivera, R. F. Vázquez Bautista, and L. J. Morales Mendoza, "Máquina de Rehabilitación de Tobillo: prototipo virtual y físico," in *Proceedings of the 10th Congreso Internacional sobre Innovación y Desarrollo Tecnológico (CIINDET '13)*, vol. 1, Cuernavaca Morelos, México, March 2013.

[5] M. Fliess, J. Lévine, P. Martin, and P. Rouchon, "Flatness and defect of non-linear systems: introductory theory and examples," *International Journal of Control*, vol. 61, no. 6, pp. 1327–1361, 1995.

[6] M. Fliess and R. Marquez, "Continuous-time linear predictive control and flatness: a module-theoretic setting with examples," *International Journal of Control*, vol. 73, no. 7, pp. 606–623, 2000.

[7] J. Linares-Flores and H. Sira-Ramírez, "DC motor velocity control through a DC-to-DC power converter," in *Proceedings of the 43rd IEEE Conference on Decision & Control*, vol. 5, pp. 5297–5302, Nassau, Bahamas, December 2004.

[8] H. Sira-Ramírez and S. K. Agrawal, *Diĕerentially Flat Systems*, Marcel Dekker, Inc, 2004.

[9] P. Thounthong, S. Pierfederici, J.-P. Martin, M. Hinaje, and B. Davat, "Modeling and control of fuel cell/supercapacitor hybrid source based on differential flatness control," *IEEE Transactions on Vehicular Technology*, vol. 59, no. 6, pp. 2700–2710, 2010.

[10] M. Jörgl and H. Gattringer, "Dynamical modeling and flatness based control of a belt drive system," *Proceedings in Applied Mathematics and Mechanics*, vol. 14, no. 1, pp. 887–888, 2014.

[11] P. Thounthong and S. Pierfederici, "A new control law based on the differential flatness principle for multiphase interleaved DC–DC converter," *IEEE Transactions on Circuits and Systems II: Express Briefs*, vol. 57, no. 11, pp. 903–907, 2010.

[12] M. Fliess, J. Lévine, P. Martin, and P. Rouchon, "A Lie-Bäcklund approach to equivalence and flatness of nonlinear systems," *IEEE Transactions on Automatic Control*, vol. 44, no. 5, pp. 922–937, 1999.

[13] M. A. Danzer, J. Wilhelm, H. Aschemann, and E. P. Hofer, "Model-based control of cathode pressure and oxygen excess ratio of a PEM fuel cell system," *Journal of Power Sources*, vol. 176, no. 2, pp. 515–522, 2008.

[14] A. Gensior, H. Sira-Ramirez, J. Rudolph, and H. Guldner, "On some nonlinear current controllers for three-phase boost rectifiers," *IEEE Transactions on Industrial Electronics*, vol. 56, no. 2, pp. 360–370, 2009.

[15] E. Song, A. F. Lynch, and V. Dinavahi, "Experimental validation of nonlinear control for a voltage source converter," *IEEE Transactions on Control Systems Technology*, vol. 17, no. 5, pp. 1135–1144, 2009.

[16] F. U. Syed, M. L. Kuang, M. Smith, S. Okubo, and H. Ying, "Fuzzy gain-scheduling proportional–integral control for improving engine power and speed behavior in a hybrid electric vehicle," *IEEE Transactions on Vehicular Technology*, vol. 58, no. 1, pp. 69–84, 2009.

[17] T. Rabbani, S. Munier, D. Dorchies, P.-O. Malaterre, A. Bayen, and X. Litrico, "Flatness-based control of open-channel flow in an irrigation canal using SCADA," *IEEE Control Systems Magazine*, vol. 29, no. 5, pp. 22–30, 2009.

[18] S. K. Agrawal, K. Pathak, J. Franch, R. Lampariello, and G. Hirzinger, "A differentially flat open-chain space robot with arbitrarily oriented joint axes and two momentum wheels at the base," *IEEE Transactions on Automatic Control*, vol. 54, no. 9, pp. 2185–2191, 2009.

[19] K. Hassani and W.-S. Lee, "Optimal tuning of linear quadratic regulators using quantum particle swarm optimization," in *Proceedings of the International Conference on Control, Dynamic Systems, and Robotics (CDSR '14)*, Paper no. 59, Ottawa, Canada, May 2014.

[20] F. L. Lewis, *Optimal Feedback Control: Practical Performance and Design Algorithms for Industrial and Aerospace Systems*, UTA Research Institute The University of Texas at Arlington, USA, 2012.

[21] G.-R. Yu and R.-C. Hwang, "Optimal PID speed control of brush less DC motors using LQR approach," in *Proceedings of the IEEE International Conference on Systems, Man and Cybernetics (SMC '04)*, pp. 473–478, Hague, The Netherlands, October 2004.

[22] M. Ruderman, J. Krettek, F. Hoffmann, and T. Bertram, "Optimal state space control of DC motor," in *Proceedings of the 17th IFAC World Congress*, International Federation of Automatic Control, Seoul, Republic of Korea, July 2008.

[23] L. B. Prasad, B. Tyagi, and H. O. Gupta, "Optimal control of nonlinear inverted pendulum system using PID controller and LQR: performance analysis without and with disturbance input," *International Journal of Automation and Computing*, vol. 11, no. 6, pp. 661–670, 2014.

[24] J.-J. E. Slotine and W. Li, *Applied Nonlinear Control*, Prentice Hall, 1991.